Materials Research Proceedings 41 (2024) 706-714 https://doi.org/10.21741/9781644903131-78

# Analysis of mechanical properties of stainless steel small diameter cold drawn wires

VAISSETTE Julien[1,a], MABRU Catherine[1,b] and PAREDES Manuel[1,c *]

[1] ICA, Université de Toulouse, UPS, INSA, ISAE-SUPAERO, MINES-ALBI, CNRS, 3 rue Caroline Aigle, 31400 Toulouse, France

[a]vaissett@insa-toulouse.fr, [b]catherine.mabru@isae-supaero.fr, [c]paredes@insa-toulouse.fr

**Keywords:** Residual Stress, Cold Drawing, Characterization, Small Diameter Wire

**Abstract.** Wire suppliers commonly only commit to the chemical composition and minimum mechanical resistance of their wires in their material certificates. Unfortunately, the cold drawing process induces residual stresses that potentially have a strong impact on the overall behavior of the wire. An explanation of the difference between the industrial 'tensile modulus' and 'flexural modulus' whereas the material has a unique 'Young Modulus' is proposed by mean of FEA and experimental tests. Moreover, in order to better estimate the complex material state of small wires (with a diameter smaller than one millimeter) a novel experimental approach has been developed to estimate the residual stress.

## Introduction

Small cold drawn wires are extensively used in mechanical systems. Some material with structural effects can exhibit flexural modulus and tensile modulus that can differ from the Young Modulus such as composite materials [1].

The elongation of grains and reduction in diameter during drawing impart a needle-like shape to the wire's grains, resulting in pronounced microstructural anisotropy between cross-sections and longitudinal views, as clearly shown in Fig. 1 [2]. This inherent anisotropy suggests potential differences in mechanical properties, specifically in flexural and tensile moduli.

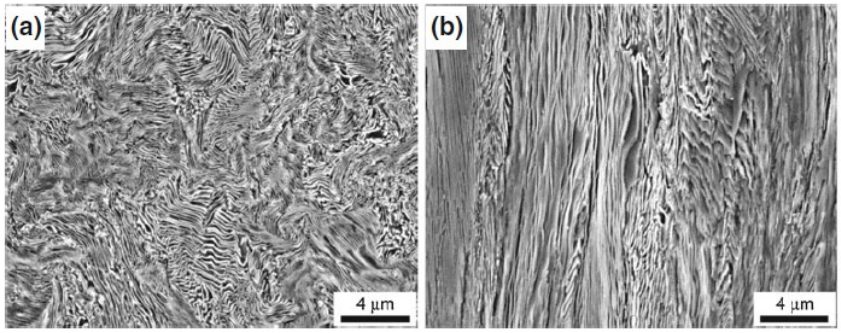


*Figure 1: Anisotropy between the cross-sectional area (a) and the longitudinal cross-section (b) of a drawn wire [2].*

Moreover, the drawing process can induce axial residual stresses in the wire [3], creating a complex stress state within the material as shown in Fig. 2.

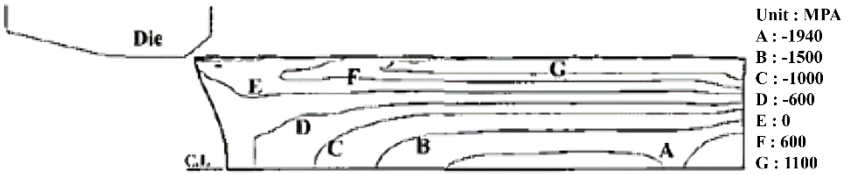


*Figure 2: Gradient of residual axial stress after drawing [3].*

Detailed studies using X-rays and Neutron diffraction reveal surface tension and central compression in drawn wires post-drawing [4] (see Fig. 3). Other methods of characterization of residual stresses exist (incremental drilling method [5] or the Sachs method [6] for instance), they are all difficult to apply on wires with small diameters: for diameters inferior to 2 mm, longitudinal drilling in the wire is extremely difficult.

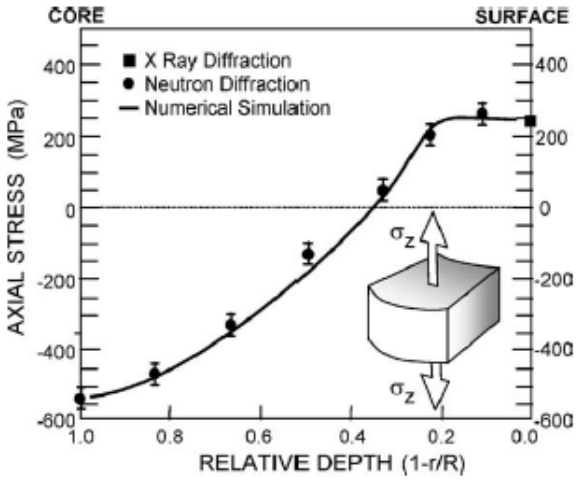


*Figure 3: Evolution of axial stress after drawing [4].*

These residual stresses, combined with grain deformation, potentially impact the structural behavior of small cold drawn wires. In order to show why manufacturers and engineers commonly use tensile and flexural moduli instead of a unique Young Modulus, a finite element study that highlights the behavior of a small cold drawn wire in a bending test is first presented. Then a novel approach to estimate the residual stress is described. Afterwards, conclusions are presented.

The aim of this work is to gain a better understanding of residual stresses in drawn wires, for use in spring production. In so doing, this work delves into an area hitherto little studied by spring manufacturers, to improve the control of dimensional tolerances of their springs.

**Study of the bending properties**

Many mechanical components as springs use small mechanical drawn wires. Small drawn wires undergo manufacturing processes that alter their mechanical properties. While manufacturers often designate distinct elastic moduli for tension and bending in wires smaller than one millimeter, scientific consensus recognizes the Young modulus as the fundamental measure. This finite element study aims to elucidate the drawing process and bending mechanisms, explaining why wires might exhibit lower stiffness than anticipated via the common Young Modulus, leading to the prevalent use of a specialized elastic modulus in bending.

The model first simulates an approximate drawing process to modify the material state and include residual stress into the wire. Compared to the real process, in the simulation the wire is drawn in one step and without temperature effect. The numerical simulation model involves

forcing a 0.84 mm diameter wire through a 0.80 mm diameter die. As for the bending test, the center distance between the fixed supports is 22.3 mm, their diameter is 3 mm and the diameter of the mobile support is also 3 mm.

The FEA is performed with Abaqus Standard (implicit), C3D20R elements (A 20-node quadratic brick, reduced integration) and 12 elements in diameter. A plane symmetry is exploited to decrease the computing time. The mesh is illustrated in Fig. 4 and the material properties are presented in Table 1. The simulation exploits multilinear kinematics hardening in order to simulate the Bauschinger effect (not the same behavior in compression and in tension) [6].

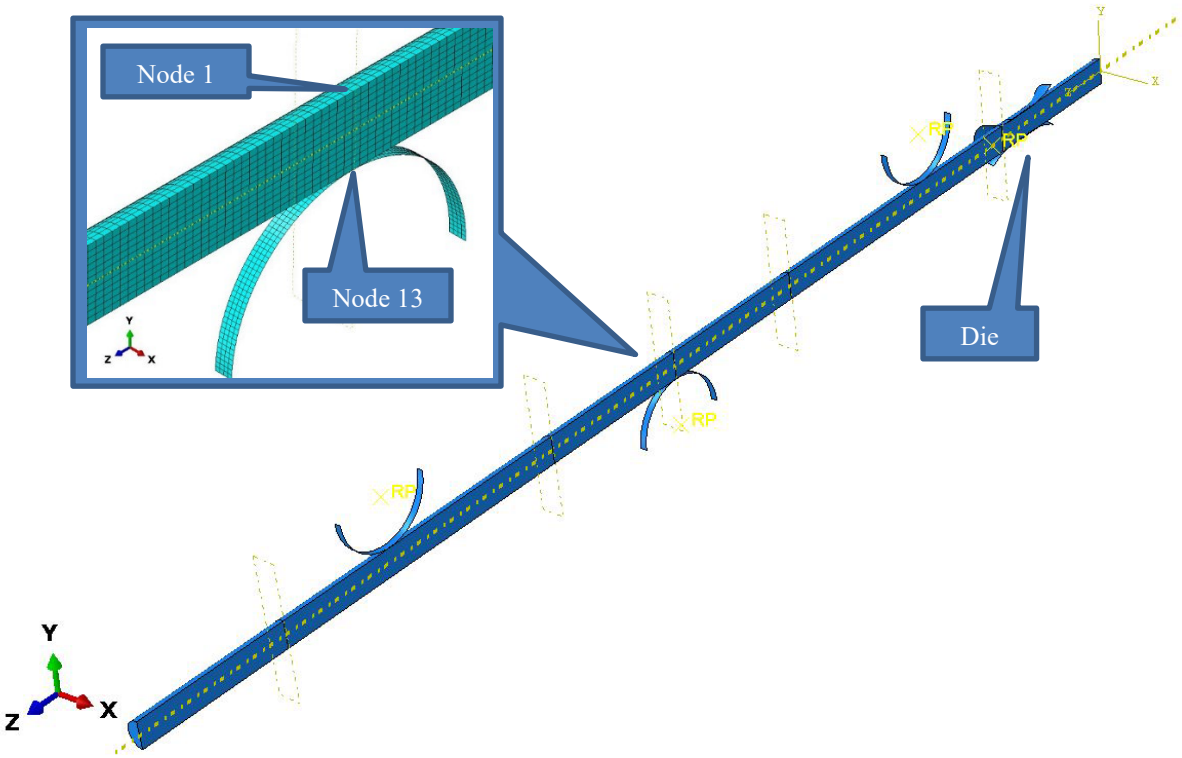


*Figure 4: Finite element model.*

*Table 1: Material properties*

| Stress (MPa) | Plastic strain | Young Modulus (GPa) | Poisson coefficient |
|---|---|---|---|
| 1000 | 0 | 165 | 0,28 |
| 2030 | 0,0072 | | |
| 2070 | 0,0108 | | |
| 2080 | 3 | | |

The common formula of mechanics of materials (Euler–Bernoulli equation for beam bending) is be exploited on the linear behavior of the load/deflection curve to identify the flexural modulus $E_f$. As expected, the obtained flexural modulus without drawing is equal to the Young Modulus $E_f$= 165 GPa = E. Moreover, the flexural modulus after drawing is lower than the Young Modulus $E_f$ = 122 GPa < E. Nevertheless, the bending curve has a linear rate that corresponds to a lower value.

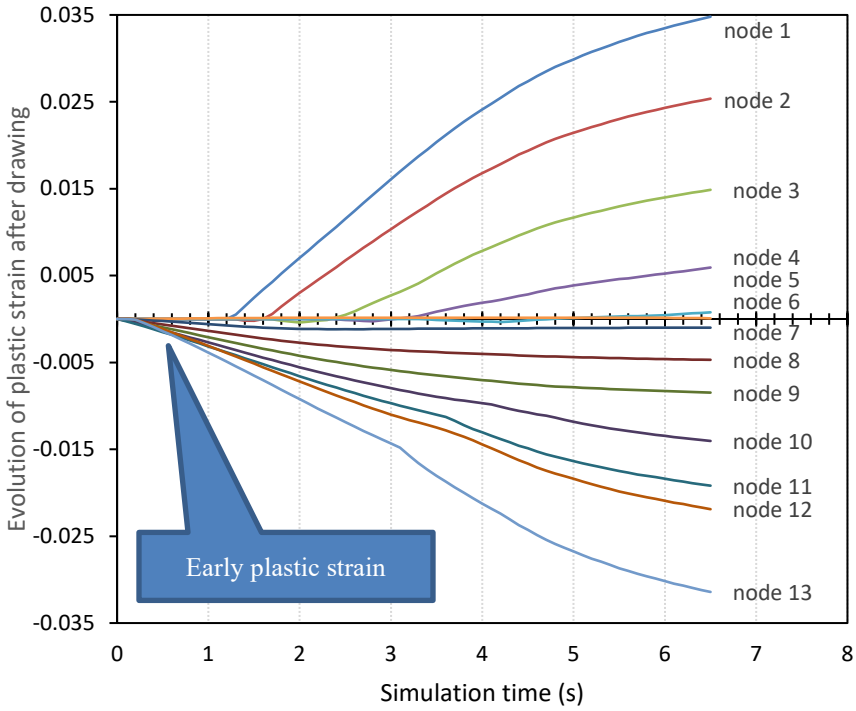


*Figure 5: Evolution of plastic strain in a bending test after drawing.*

In order to explain this phenomenon, the evolution of plastic strain on a section all along the test has been plotted (see Fig. 5). The initial state after drawing is set as a reference. In a common bending test one half of the wire is in tension, the other one is in compression and the center is neutral. When the bending test begins, the wire is first in an elastic state and there is no plastic strain. Then, at a given level of external load, plastic strain appears at the external surface and progresses to the center of the wire. We can see this evolution on the upper part of Fig. 5 which is dedicated to the half of the wire in tension (positive values of plastic strain). Node 1 is at the external surface and after about 1.2 seconds of simulation time, first yielding occurs and the plastic strain progresses towards the center (node 7).

In a bending test of a material supposed to be linear elastic, homogeneous and isotropic, the behavior is the same in the compression state of the wire but it is not the case here. As shown in Fig. 5, because of the drawing process (and thanks to the multilinear kinematic hardening simulation that considers the Bauschinger effect), early plastic strain directly appears at the beginning of the test in the part of the wire in a compression state (negative values of plastic strain). This area is highlighted by an arrow in Fig. 5 (nodes 8 to 12 are involved, except node 13 at the surface which is in a preliminary tension state due to the prestress). Thus, at the beginning of the test, even when the global bending behavior of the wire is linear, a part of the section is plastically deformed. We know that the material in increasing plastic state has a lower stiffness. As a consequence, the whole stiffness of the section is decreased and that explains why the calculated flexural modulus is lower than the Young modulus. From a scientific point of view, a small cold drawn wire is no more a uniform material but could be considered as a complex structure.

**Estimate of the residual stress**

The previous FEA simulates a simplified drawing process. This simulation enables to highlight the axial residual stress after drawing (Fig. 6). As previously shown, the external surface is in tension and the core is in a compression state.

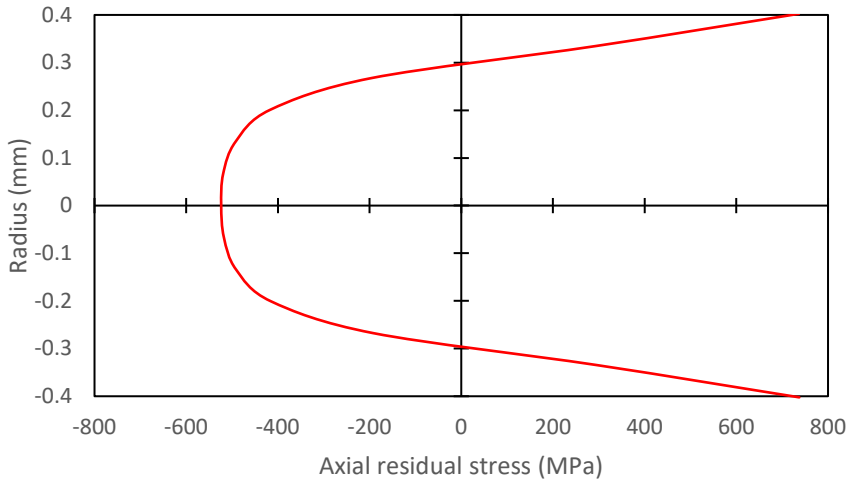


*Figure 6: Axial residual stress state in the section of a 0.8mm diameter wire (FEA).*

Unfortunately, the common approaches to evaluate the residual stress are not directly available for small wires. For that reason, we propose a new approach based on material removal. The experimental approach [8] consists in removing a part of the material by coating the wire in a soluble resin and then gently polishing the sample in order to make a flat cut parallel to the wire axis. After resin dissolving, the new curvature is measured as described in Fig. 7.

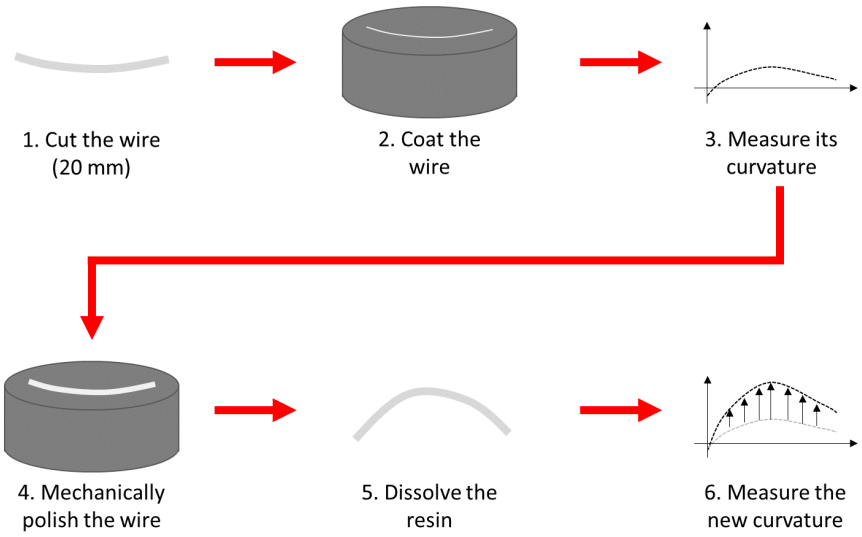


*Figure 7: Experimental steps of the matter removal method for small wires.*

The curvature measurement is not trivial when dealing with small wires. In our case, curvature measurements were performed on Alicona InfiniteFocusSL, an optical 3D measurement device. Once the curvature is measured, the next step consists in an analytical approach to estimate the residual stress state. This approach has been inspired by the work of Han et al.for ultra-thin plate-shaped optical parts [9]. The idea is to propose an analytical formula for the residual stress shape and then to find the parameters values that will induce the experimental curvature previously found.

Before material removal, the residual stress induces a global equilibrium in the wire. After matter removal the initial equilibrium vanishes and a new equilibrium is found that induces a

curvature of the wire. This curvature can be linked to the bending momentum $M_b$ induced by the removed residual stress.

$$M_b = \frac{a}{b^2} 2EI \quad (1)$$

Where a is the maximal radial displacement, b is the mean axial distance, I is the area moment of inertia after matter removal and E the Young modulus.

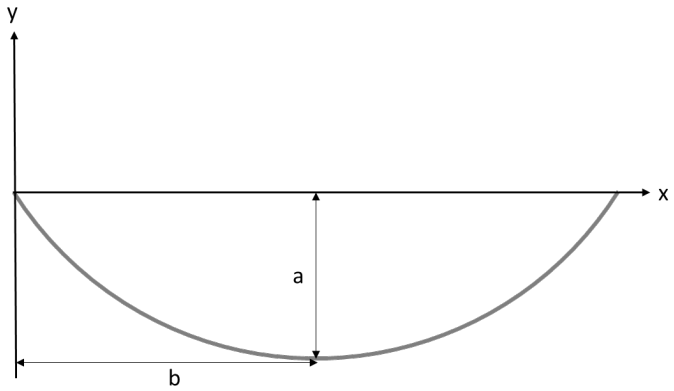


*Figure 8: wire profile after matter removal.*

The next step involves evaluating the residual stress in the wire. First of all, a residual stress profile is proposed that can fit the profile shown in Fig. 6.

$$\sigma_0(r) = A\left[-\cos\left(\pi\left(\frac{|r|}{R}\right)^n\right) + B\right] \quad (2)$$

with:
A, n, B: parameters to be defined
R: wire radius
r: radial coordinate, between -R and R.

In order to find the unknown parameters, we need to study the wire equilibrium before and after matter removal. We know that before matter removal the wire is in equilibrium. Thus, the following equation is satisfied:

$$\iint \sigma_0(r)\, dS = 0 \quad (3)$$

We also know that the removal of a part of the wire induces $M_b$. Thus:

$$M_b = \int y' \sigma_0(r) dS \quad (4)$$

Where y' is the coordinate in the wire normal to the cut as illustrated in Fig. 9

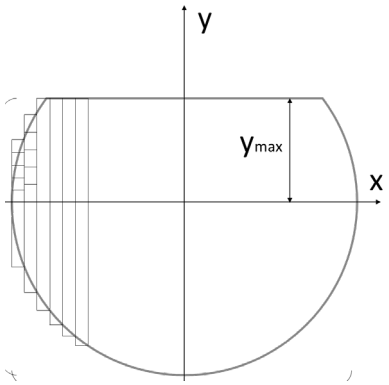


*Figure 9: wire section after matter removal.*

We consequently have 2 equations to be satisfied but 3 parameters to be found. In order to solve this problem, we chose to fix the radial coordinate where the radial stress is null (0.3mm in the case illustrated in Fig. 6). The parameters values are finally determined using a short optimization algorithm.

In an application example, a stainless-steel AISI 302 wire (0.8mm diameter, E=185 GPa) has been tested. The experimental measurements induce a= 0.078mm, b=5mm and $y_{max}$ = 0.23mm (see Fig.11). Thus I'=0.01167mm$^4$ and $M_b$ = 13.47 N.mm. The solving process enables to estimate the equation for the axial residual stress and illustrated in Fig. 10:

$$\sigma_0(r) = 865\left[-\cos\left(\pi\left(\frac{|r|}{0{,}4}\right)^{2{,}93}\right) + 0{,}216\right] \quad (4)$$

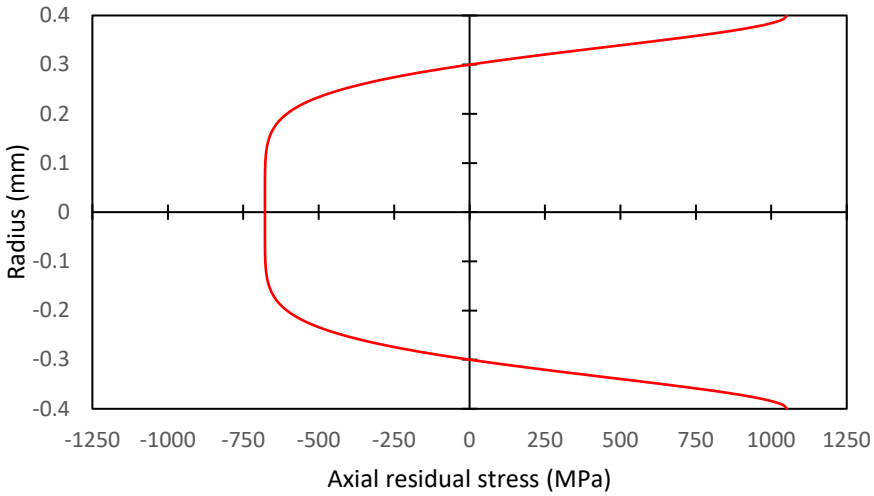


*Figure 10: Evaluation of the axial residual stress in the wire.*

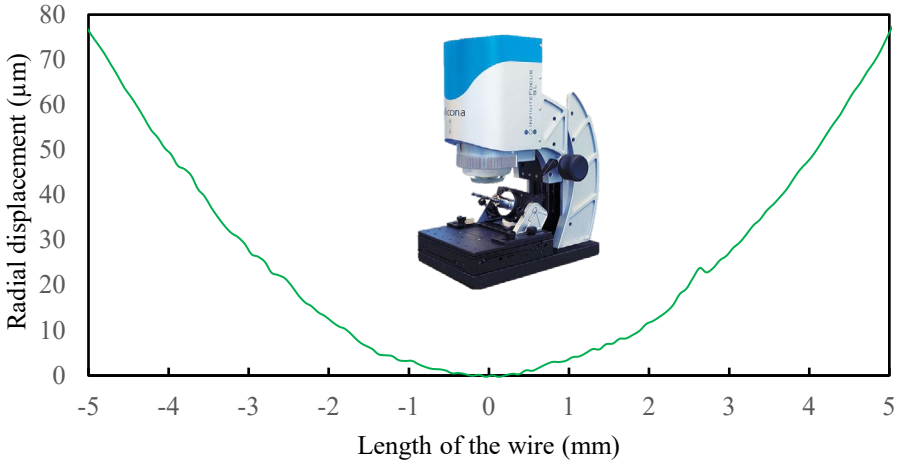


*Figure 11: Radial displacement measured after the removal of a 0.17 mm layer, on a 0.8 mm diameter wire.*

It is important to point out that the analytical estimate of residual stress intensity seen in Fig.10 cannot be directly compared with that obtained after numerical simulation of a wire simplified drawing operation in Fig. 6. Indeed, the latter simulation is not quantitatively objective, since it studied residual stress intensity after a wire drawing operation not fully representative of the 0.8 mm diameter wire drawn here. The two curves can therefore only be compared qualitatively.

## Conclusions

The aim of this paper was to delve into the mechanics involved in both the drawing process and bending to clarify why a wire might exhibit a softer behavior than anticipated by its Young modulus. Additionally, it sought to estimate the residual axial stresses.

A simplified Finite Element Analysis of the drawing process helped gauge the material's state upon delivery to manufacturers. Subsequently, the simulation extended to a bending test. In-depth simulation analysis revealed that the loss of stiffness of the linear behavior was due to substantial plastic deformation during drawing, particularly an inner portion of the wire undergoing direct plastic compression upon the onset of the bending test. This localized plasticity beneath the surface, despite the wire's overall linear behavior, contributed to a decreased overall stiffness, necessitating the use of a specific elastic modulus in bending for a consistent equivalence.

Furthermore, an innovative experimental method was developed to characterize residual stresses, tailored for small wires (diameter less than 1 mm). The method involved coating the wire in a soluble resin, followed by gentle polishing to create a flat cut parallel to the wire axis. Similar to other residual characterization methods, the goal was to observe the deformed shape resulting from the release of residual stress post-polishing. an analytical approach was employed to estimate the magnitude of the residual stress causing the curvature change.

Experiments performed on a 0.8 mm diameter AISI 302 wire revealed remarkably high residual stress intensity, underscoring the necessity for a thorough characterization of residual stress profiles in cold-drawn wires. However, further research is required to refine the initial estimate of the radius where axial residual stress is null.

## References

[1] T.-I. Lee, C. Kim, M. S. Kim, T.-S. Kim, Flexural and tensile moduli of flexible FR4 substrates, Polym. Test., 53 (2016) 70-76. https://doi.org/10.1016/j.polymertesting.2016.05.012

[2] J. Atienza, J. Ruiz-Hervias, M. Elices, The Role of Residual Stresses in the Performance and Durability of Prestressing Steel Wires, Exp. Mech., 52, (2012) 881-893. https://doi.org/10.1007/s11340-012-9597-1

[3] S.-K. Lee, H. H., K. M., B. M., Influence of Process Parameters on Residual Stress and Reducing Residual Stress in Drawn Wire, Trans. Mater. Process.,14 (2005) 704-711. https://doi.org/10.5228/KSPP.2005.14.8.704

[4] J. M. Atienza, J. Ruiz-Hervías, M. Martinez-Perez, F. Mompeán, M. García-Hernández, M. Elices, Residual stresses in cold drawn pearlitic rods, 52-4 (2005) 305-309. https://doi.org/10.1016/J.SCRIPTAMAT.2004.10.010

[5] G. Montay, O. Sicot, A. Maras, et al. Two Dimensions Residual Stresses Analysis Through Incremental Groove Machining Combined with Electronic Speckle Pattern Interferometry. Exp Mech 49 (2009) 459–469. https://doi.org/10.1007/s11340-008-9151-3

[6] A. P. Parker, A critical examination of Sachs' material-removal method for determination of residual stress, J. of Pressure Vessel Technology, 126 (2004) 234-236. https://doi.org/10.1115/1.1689357

[7] W. M. Stobbs, S. Paetke, The Bauschinger effect in cold drawn patented wire, Acta Metall., 33- 5 (1985) 777-783. https://doi.org/10.1016/0001-6160(85)90101-4

[8] Julien Vaïssette, Manuel Paredes, Catherine Mabru, A residual stress characterization method by matter removal of a small diameter wire, 11th International Conference on Residual Stresses - Nancy – France – 27-30th March 2022

[9] X. Han, Z. Jin, Q. Mu, L. Niu, P. Zhou, Internal stress and deformation analysis of ultra-thin plate-shaped optical parts in thinning process, Opt. Express, 27-19 (2019) 27202-27214. https://doi.org/10.1364/OE.27.027202